AUTONOMOUS SPACE PROCESSOR FOR ORBITAL DEBRIS

UNIVERSITY OF ARIZONA

This work continues to develop advanced designs toward the ultimate goal of a GETAWAY special to demonstrate economical removal of orbital debris using local resources in orbit. The fundamental technical feasibility was demonstrated in 1988 through theoretical calculations, quantitative computer animation, a solar focal point cutter, a robotic arm design, and a subscale model. Last year improvements were made to the solar cutter and the robotic arm. Also performed last year was a mission analysis that showed the feasibility of retrieving at least four large (>1500-kg) pieces of debris. Advances made during this reporting period are the incorporation of digital control with the existing placement arm, the development of a new robotic manipulator arm, and the study of debris spin attenuation. These advances are discussed here.

INTRODUCTION

We can hardly improve upon the lucid descriptions of the orbital debris issue by science writers[1-4] and other popular news media coverage[5-9]. Without doubt, the problems of orbital debris have grown to be of serious concern to astronomers, space technologists, and to terrestrial dwellers. The specific problems were presented at the 39th IAF Congress. The University of Arizona Space Engineering Design team is developing the design for economical removal of the larger debris pieces through local resource utilization. The fundamental idea is to concentrate solar energy into a point focus, cut the debris into precise shapes that can be added on to the "sweeper" craft, and robotically assemble the pieces into a manageable configuration. This is followed by one of three disposal modes: (1) retrieval by a spacecraft (STS, HERMES, BURAN, etc.), (2) precise ocean splashdown, or (3) planned burnup upon atmospheric reentry. The fundamental space technologies to be demonstrated are solar cutting of candidate space debris materials, robotic assembly, and accurate disposal. In 1988 the University of Arizona began participation in the USRA program and demonstrated solar cutting and a subscale model robotic arm. In 1989, a full-scale robotic arm with manual controls was developed and the solar cutter/robotic arm assembly was shown to be technically feasible. Also in 1989, a mission analysis was performed in which the large debris environment was identified and a four-debris retrieval sample mission analysis showed the propellant requirements to be well within reason. This year, 1990, the existing robotic arm was converted to digital control using an IBM PC, a second robotic arm was developed for precise pick and place operations, and the problem of debris tumbling was addressed and various detumbling methods were investigated. This report is a summary of the work and explains the details of space engineering.

Consistent with the USRA philosophy, new undergraduate students were involved in the design process. This year, 11 new students were involved in the Autonomous Space Processor for Orbital Debris (ASPOD) design. The project continues to draw worldwide attention including correspondence with elementary and high schools.

DEBRIS SPIN ATTENUATION

The purpose of this project was to research and recommend methods of attenuating the rotational spin of orbital debris so that an ASPOD satellite can safely grasp them for retrieval. To avoid possible damage to the ASPOD craft, only passive means of attenuation were investigated. The use of passive means is defined as the use of methods of attenuation that do not involve ASPOD in direct contact with space debris, thereby endangering it. Some of the design criteria and target specifications are (1) attenuate the rotation of an object spinning about one axis; (2) attenuate the rotation of an object having a mass of up to 2000 kg and rotating with rotational speeds of up to 50 rpm; (3) attenuate the rotation of an object up to 7 m in diameter and up to 7 m in height; (4) use a minimal amount of energy; (5) attenuate at least four objects per mission; (6) require no maintenance; (7) must not interfere with the normal operation of other functional satellites; (8) must not create more debris; (9) must weigh less than about 500 lb; and (10) must have a reasonable expense relative to the space industry.

Satellites and most other space debris generally contain a certain amount of rotational energy. The problem of dealing with the rotation of a large, nonsymmetric object containing a lot of mass orbiting the Earth must be solved before the satellites can be safely and effectively collected.

A workable solution dealing with debris capture must allow the rotational energy of the debris to be contained or dissipated without transferring it to the collector satellite. The space debris that is proposed for collection is often very massive, 2000 kg or more, with spin rates of up to 50 rpm. These figures suggest that there can be quite a bit of angular momentum involved.

SOLUTIONS

As a first step, various attenuation methods were researched and evaluated. Of all the methods investigated, four were chosen as possible solutions and merited further analysis. Each of these four solutions uses a different physical principle (for example, conservation of angular momentum or conservation

of energy) to accomplish the attenuation of the satellite. Although each of the four designs merits further investigation, for the present the most promising of the four was singled out for detailed analysis and testing.

Reeled weight mechanism. The physical principle used in this method is to translate the rotational energy into linear kinetic energy, then into potential energy. This design uses a reeled cable capable of attaching itself to the debris by the cable's free end. Also contained in the reel mechanism is a generator allowing the cable to reel out, turning permanent magnets around a stationary armature and storing that energy in a battery. This generator can then act as a motor by turning the stored energy in shaft power, allowing the cable to be reeled in. Once the free end of the cable is attached to the debris in its plane of rotation, the reel is then allowed to freely move away from the debris due to centrifugal acceleration, yet is still tethered by the cable. The reel will move away in a straight path while the debris continues to spin, and the attachment point of the cable on the debris will rotate with the debris, wrapping a portion of the cable around the debris. At this time the reel will create a drag force on the cable by engaging the generator and then storing that energy. Due to the centripetal force of the reel attached to the much more massive piece of debris, the reel will attempt to move into a radial position about the debris' center of mass. Before it comes near this point some of the stored energy will be used to reel the reel mechanism back into the debris, at which point the process will start over. Some of the advantages to this system are the ease of attachment to essentially any shape of debris and the relative simplicity of the mechanism. Some of the problems are the difficulty in analysis and testing of the system and the chance of the cable becoming permanently entangled in protrusions on the debris.

Coiled spring mechanism. Figure 1 presents the proposed configuration for the coiled spring mechanism. This proposed mechanism consists of a component for attaching to the debris, a ratchet, a coiled spring, and a stabilizer. The idea behind this solution is to absorb the rotational energy of the debris and store it in a coiled spring as potential energy. The purpose of the ratchet is to act as a locking mechanism for the spring when it winds up completely. Winding up the spring, though, necessitates the use of a stabilizer to hold the other end of the spring fixed. A stabilizer is thought of as a servo-controlled gyroscopic platform where gyroscopes are to be used only as sensors. The resolver (the "brain" of the control system) will be continually feeding corrections through the feedback controlled loop to keep the attachment to the platform fixed in space. The greatest advantage of this process is that it can attenuate the rotation of the debris quickly, i.e., within minutes. Furthermore, the attenuation of the debris is complete (100%). The disadvantages of this idea are the requirements for powering the gyroscopic sensors and lubricating the ratchet. Another more important problem is that the ASPOD will eventually be involved actively in the process by powering several thrusters as well as its momentum wheels. Since this may create safety problems for the vehicle itself, the idea was abandoned for the time being and our effort was concentrated on developing passive means of attenuation.
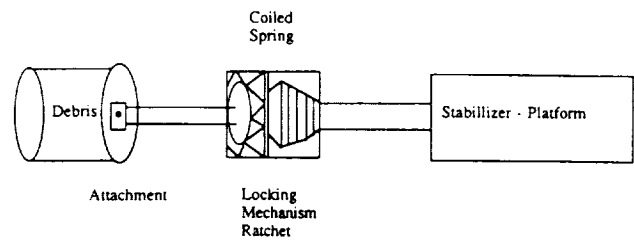

Fig. 1. Coiled Spring Mechanism

Long cable mechanism. For this design there are two ways in which it could work. One would be to let out a cable with a mass attached to the end, thereby increasing the moment of inertia and slowing the satellite down. This would not allow the satellite to come to a complete stop, but it could possibly slow the satellite down enough for a robotic arm to manipulate it. The cable would have to be cut off when maximum attenuation occurs, preferably so that it would reenter the Earth's atmosphere, because once the robotic arm attached to the satellite, the cable would reel in uncontrollably due to the momentum of the cable. The other method would be to leave the cable on for an extended amount of time and allow the gravity gradient to slow the satellite to a complete stop. The satellite could then be grabbed and the cable reeled in since the rotation of the satellite would be fully attenuated. Figure 2 shows a representation of this method.
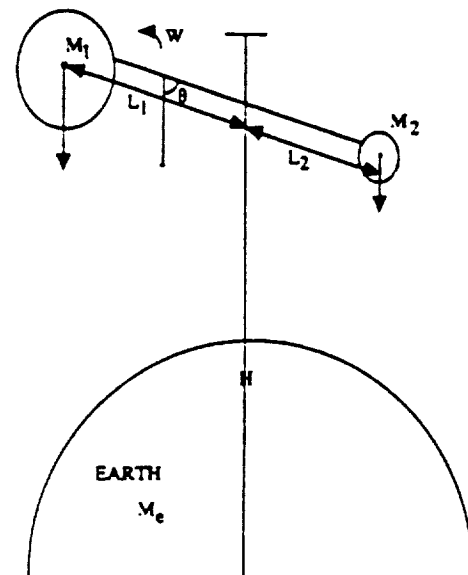

Fig. 2. Long Cable Configuration

Geared-bar mechanism. The geared-bar mechanism is the solution selected by the attenuation research group for further development and is detailed below.

Geared-bar Mechanism

Theory of operation. A representation of the gear bar can be seen in Fig. 3. The centrifugal acceleration acting on the flywheel forces the flywheel radially outward to the end of the geared bar. If the geared bar were smooth, the flywheel would just translate outward without spinning; however, the contact forces between the gear and the bar apply a torque about the center of the gear, forcing the flywheel to spin as well as translate. Mathematical analysis and experimentation show that as the angular rotation of the flywheel increases, the angular rotation of the debris decreases. A ratcheting mechanism is attached to the system so that when the flywheel reaches the end of the bar the flywheel will continue to rotate freely.

The effectiveness of our design depends on the length of the geared bar and the mass moment of inertia of the flywheel. It could happen that the configuration necessary to achieve an adequate amount of attenuation would be unfeasible to take into space due to the size and/or mass of the flywheel and the length of the bar. If this is shown to be true it should be possible to attach a motor to the flywheel and "reel" the flywheel back in, while the ratchet mechanism allows it to maintain its angular velocity and let it move out again. This process could be repeated as many times as necessary.
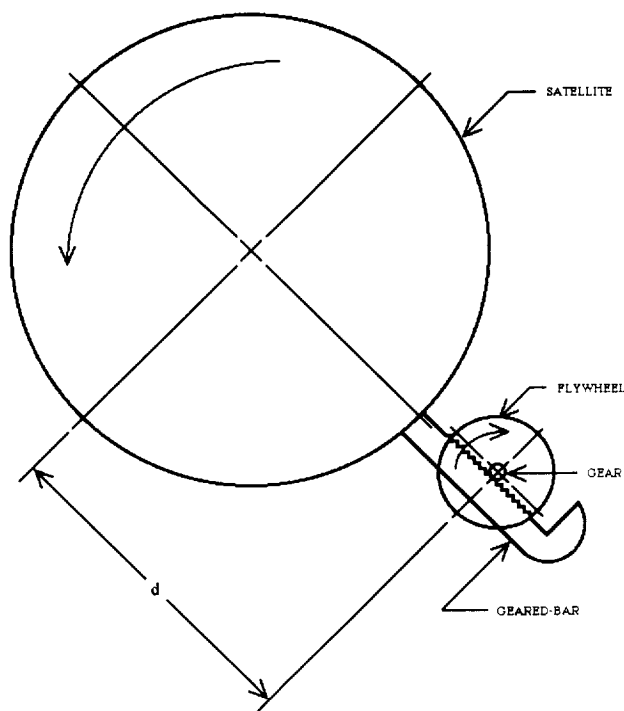

Fig. 3. Geared-bar Mechanism

Design. A rudimentary device was fabricated for experimental purposes. The design that was used included a rubber wheel and friction bar to simulate the rack and pinion system. A small cart supporting the flywheel and friction wheel with a bearing rolled along a track that represented the geared bar. The friction wheel rolled along a friction bar attached to the track forcing the flywheel to rotate. The combination of the flywheel and the cart simulated both the rotation and the translation of the flywheel. To simulate the ratcheting mechanism, the friction bar was cut shorter than the track. This allowed the flywheel to rotate freely once it reached the end of the track. This design was not adaptable to the use of a motor; however, it was felt that showing that the theory mechanism would work for one pass was sufficient to show that this method of attenuation was feasible.

Experiment. Previously, a large model representing space debris was built for attenuation experimentation purposes. This model is an octagonal solid approximately 48 in in diameter and 72 in high with a calculated mass moment of inertia of 655 lbm ft. The "debris" is attached to the ceiling and floor with a large metal rod about which it rotates. Lubricated bearings were used to minimize the frictional effects.

To gather data, a systematic process had to be developed to measure the time per revolution. A computer program was used to record the needed data. A mark was made on the "debris," which was then spun up to an appropriate speed. Each time the mark came into sight, a key was pressed on the computer. The program would then print the number of revolutions and measure the time elapsed. With this data, the program calculated the time between revolutions and revolutions per minute. Finally, this information was exported to a spreadsheet program for further analysis and graphing.

To prove the effectiveness of the geared-bar mechanism, it was necessary to find a way to separate the effects of the changing mass moment of inertia due to the flywheel translating outward vs. the effects of the rotational kinetic energy being transferred to the flywheel. To do this, reference data had to be taken. These reference data consisted of several measurements with the flywheel retracted and several with the flywheel extended. Before measurements could be taken with the geared-bar mechanism fully operational, one additional component needed to be added. Because the debris needed to be brought up to a functioning speed before the flywheel could be released, it was necessary to develop a release mechanism so that the flywheel would not begin to move before the appropriate speed was attained. This was done by including an eyelet on the flywheel, and passing a pin through it that could be easily pulled out when needed without significantly affecting the speed of the debris.

As stated above, these measurements were taken for each case: the flywheel retracted, extended, and operational. Figures 4, 5, and 6 show the relative quality of the measurements for each case and their characteristic curves.

Although the reference data were taken, a standard procedure to spin up the debris at an equal rpm for each run was not developed, nor was there a way to measure the energy added to the system. It was necessary, therefore, to determine
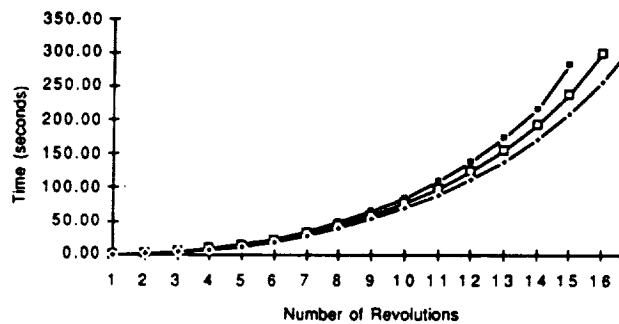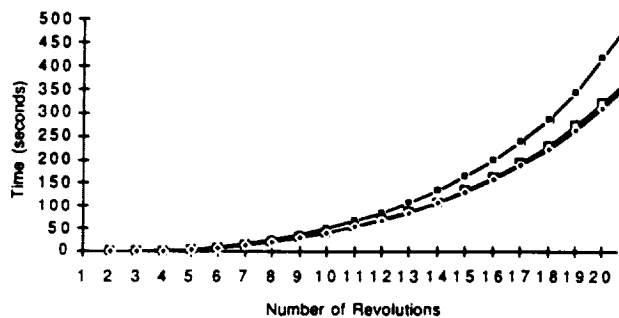
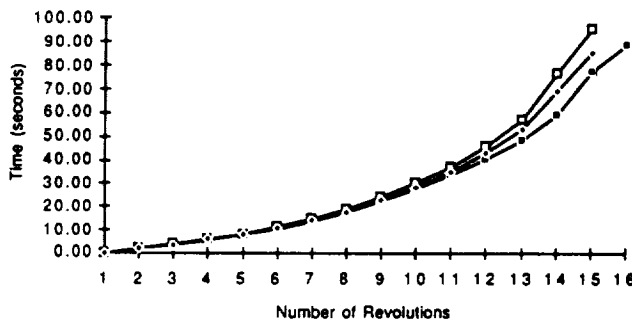Fig. 4. Flywheel Retracted

Fig. 5. Flywheel Extended

Fig. 6. Flywheel Translating

Fig. 7. Experimental Comparison

a method for comparing the data with the three different cases. Because of limitations with the graphing software used, it was felt that taking the points at which the debris came to rest with each case and counting the maximum, common number of data points backward would be a reasonable method for developing a common reference. For example, the working case only included 14 data points, so the last 14 data points for each case were used.

Figure 7 illustrates the effects between the three different cases. The line with the flywheel retracted is steep due to the low relative inertia. The line with the flywheel extended is flatter and the time of rotation longer due to the effects of increased mass moment of inertia. If the working case
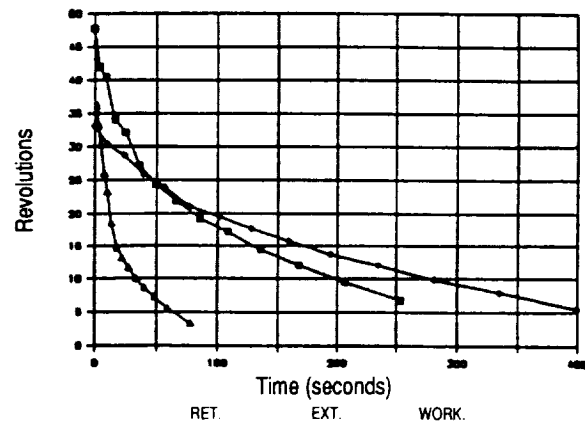
decreased the rotational speed of the debris solely due to the effects of the changing mass moment of inertia, one would expect the line for the working case to lie somewhere between the retracted and extended cases. In fact, the graph should begin at the approximate point of the retracted case because of the identical value for the mass moment of inertia and end near the same point of the extended case because the same amount of energy should still be in the system. It was not the group's goal to "prove" the effects of changing the mass moment of inertia, but to prove that the flywheel actually absorbs the energy of the debris. To confirm this, the graph of the working case should start near the point of the retracted case and end significantly below the extended case. The working case line does confirm this hypothesis.

This experiment does not exactly model the case of debris spinning in space because satellites in space are not pinned, therefore the center of rotation would change as the flywheel moves out. The mass of the flywheel could be optimized to minimize these effects. Nonetheless, this system of attenuation will still work, because the center of rotation will always lie between the centers of the debris and the flywheel, maintaining the centrifugal component of acceleration moving the flywheel outward.

In conclusion, and most importantly, the geared-bar mechanism of the experimental case does absorb the rotational energy of a spinning body. For the 3 cases mentioned above, the time for the last 14 data points is 253 sec for the retracted case, 400 sec for the extended case, and 59 sec for the working case. The above experiment also proves that the attenuation is not solely due to the change in mass moment of inertia, but actually performs a significant amount of energy transfer.

Computer modeling. In order to investigate the dynamics of the geared-bar mechanism as an attenuator of the rotational energy of a satellite, several approximations to the actual case were considered. The first case, consisting of the two-dimensional analog (Fig. 8) of the actual case (Fig. 9), assuming perfect targeting and neglecting the attachment phase and the endpoint locking of the flywheel, was solved analytically.
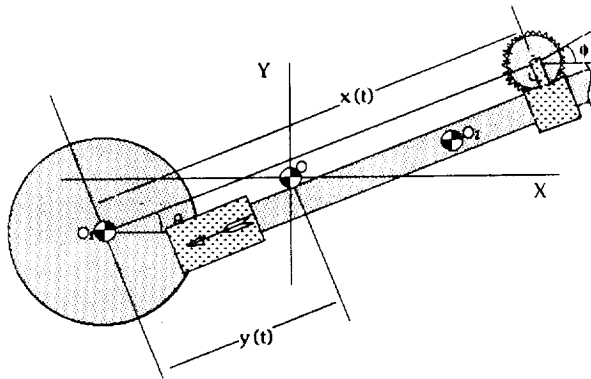
Fig. 8. Attachment Parameters

Total angular mom. vector
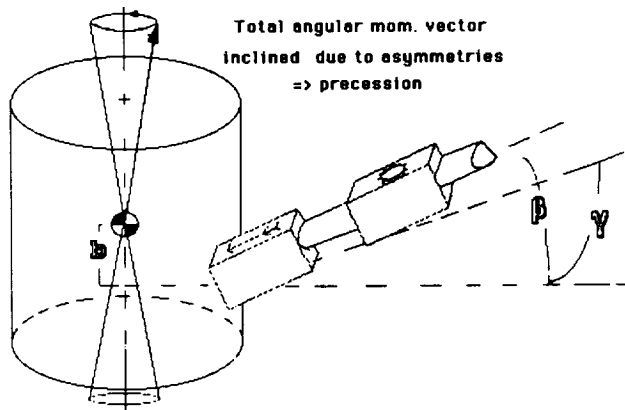inclined due to asymmetries
=> precession

Fig. 9. Attachment Sensitivities

Under the above assumptions, the analysis suggested that an attenuation of about 50% could be attained for a rack length of 4 m, and an operation of 50 sec. These results pertain to a satellite modeled as a 2000-kg cylinder, 4 m in height and 3 m in radius rotating at 50 rpm. The 40-kg flywheel used in the analysis was 1 m in diameter, while the rack was assumed weightless. At this point it should be mentioned that the attenuation effects are highly dependent on the inertial properties of the satellite. Thus, it should be kept in mind that the diversity of satellites to be attenuated adds to the complications and limits the applicability of the design.

In order to investigate the effects of the geared-bar attenuator when it is not attached at right angles to the principal axis of rotation of the debris, as well as when it is attached off-center with respect to the satellite's center of mass (Fig. 9), an analysis was attempted on a software package available at the University of Arizona. This software facilitated a three-dimensional analysis and made it possible to animate the resulting effects, for visual and demonstrational purposes. For a satellite with inertial properties as mentioned above, the software shows attenuation as high as 70% during the first 5 sec for the two-dimensional case, but not more than 25% for the three-dimensional case that involves geometrical

asymmetries and precessions. The fact that the rack and pinion joint is not 100%, as was assumed by the software, will lengthen the time needed for attenuation. Figures 10 and 11 show the angular velocity of the debris for the two- and three-dimensional cases respectively.

The results indicate that the targeting and alignment of our device is essential, and therefore a process of determining the center of mass of the debris before operation is essential. The software can provide results once the device is attached to the satellite; however, impact forces caused by the attachment process were not modeled.

To evaluate the model, a final comment on the effects upon impact needs to be made. Provided that no eccentric forces are present, i.e., perfect targeting, any components directed radially from the Earth will cause oscillations that are estimated to die out. Moreover, any angular components will result in shifting the orbit but not changing the orbit altitude. Thus, the effects on the debris will be mostly translational and will not greatly affect the attenuation process.
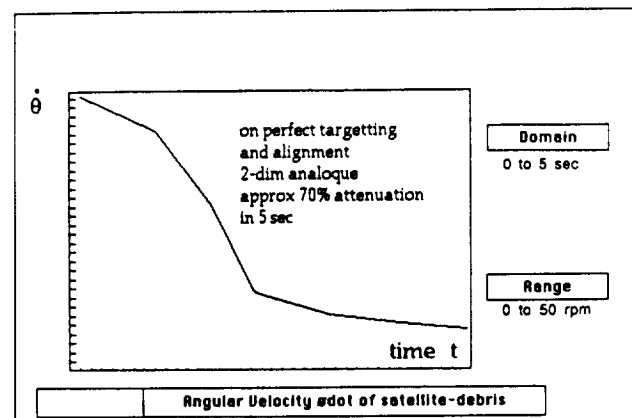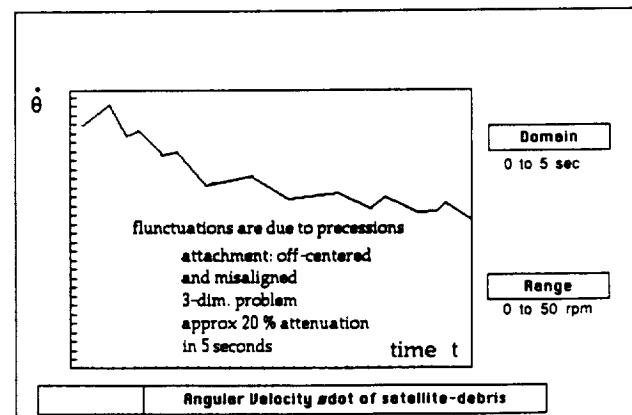

Fig. 10. 2-D Computer Modeling

Fig. 11. 3-D Computer Modeling

Attachment. Since the purpose of this project was to test processes for attenuation, the issue of attaching the mechanism to the satellite was not initially addressed. However, it was felt that developing a method of attachment was necessary to complete the subject of attenuating the rotational motion of orbital debris.

Several ideas were considered. Wrapping something around the satellite (similar to lassoing) was discarded because it could not be guaranteed that there would be a perfectly clear path all the way around every satellite due to auxiliary objects such as antennas. Grabbing the satellite was felt to be impractical because the skin of the satellite is very flimsy (since its only purpose is to shield the inside from solar radiation and small particles) and could not sustain very large forces and moments.

The conceptual design of the device that was chosen to build was much like an umbrella. The device would pierce the skin of the satellite and, once inside, open up to prevent the device from slipping back out.

As can be seen in Fig. 12, a motor turns a threaded rod and the collar with the shorter links attached begins to move. Once the collar contacts the back-plate the collar no longer moves along the threaded rod and the shorter links then pull the larger links until both are at right angles to the threaded rod. The mechanism would have worked with only the longer rods; however, the design chosen minimizes the load that each link has to take and increases the mechanical advantage of each link, thereby requiring less energy.

The motor to drive the threaded screw would be a DC motor. The batteries would be charged prior to use using the power source available to ASPOD.

Conclusion. The overall purpose of this part of the project was to research and design a mechanism that would slow or attenuate the rotation of a satellite. The solution found would involve launching a geared-bar mechanism to the piece of debris. The tip would pierce the skin and six links would then open up to keep the device in place. The flywheel would then be disconnected from its locked position and allowed to rotate out. This would transfer the rotational energy from the satellite

to a more manageable form in the flywheel. This method was proven to work through experimentation and mathematical and computer analysis.

DIGITAL CONTROL OF PLACEMENT ARM

The ASPOD design incorporates a solar-powered metal cutter to facilitate dead satellite processing in a cost-effective manner. In order to position debris at the focal point it is necessary that the ASPOD be equipped with robotic arms. The arm function is to hold and move material to be cut in the focal plane of the solar concentrator. After this initial development stage, the gathering arm was controlled with a variable-speed on/off control panel. In order to automate the arm and to better simulate its operation in space, a hardware/software controller was designed. The objective of the digital control was to eliminate the direct human interface initially needed to operate the arm and to replace it with a software interface that would accept commands entered into a PC terminal. The digital control would increase the accuracy of the arms' movements, and with the software interface a program could be developed in order to perform a pick-and-place operation or a more defined cutting operation.

Design Specifications

The robotic arm has five revolute joints as shown in Fig. 13 with axes and degrees of joint rotation. The most important component of the whole robot system is the digital control system whose components are a power supply, voltage regulator, two motion controller boards (from Motion Engineering), five motor drivers, five optical encoders, five DC motors, and an IBM PC. Two of the hardware parts—the power supply and the motor driver—required custom design and fabrication. These components were constructed by members of the team.

The hardware needed to build the power supply included a transformer, a bridge, and two capacitors to produce a dual output of +25 V/-25 V with a smooth signal (resembling DC voltage). The +25 V was also connected to a voltage regulator to produce +5 V for the optical encoder. Figure 14 shows the circuit design for both the power supply and the voltage regulator.

Five individual motor drivers (channels) were built within the motor driver. Each driver consisted of a high-voltage operational amplifier to amplify the input voltage from motion controller boards, transistors, capacitors, and resistors (see Fig. 15). The motor driver receives a voltage from the motion controller board between -10 V/+10 V. The operational amplifier amplifies the voltage at values of +20 to -20 V. The transistor amplifies the current and then sends a voltage to drive the DC motors at each joint of the arm.

The optical encoders (HEDS-5600) are used to provide accurate motion detection. They provide a high-performance, optical incremental encoder that emphasizes high reliability and resolution, low cost, and ease of assembly. The optical encoders were attached at the points of rotation to measure the angle of rotation at each joint, and required a rigid mount and modification to the shaft at each joint.
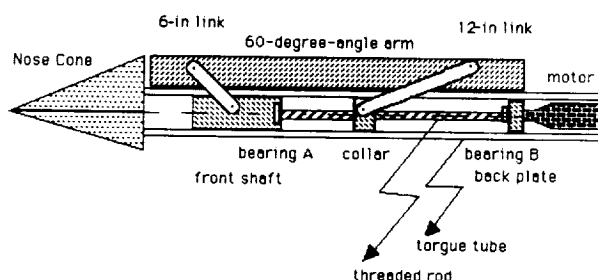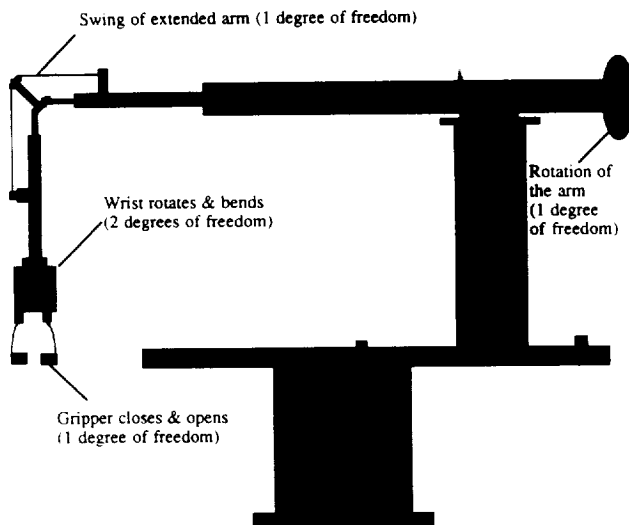

Fig. 12. Attachment Device

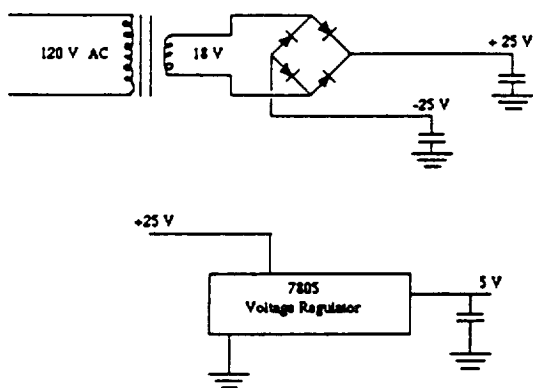Fig. 13. Robotic Arm Showing Degrees of Freedom at Joints
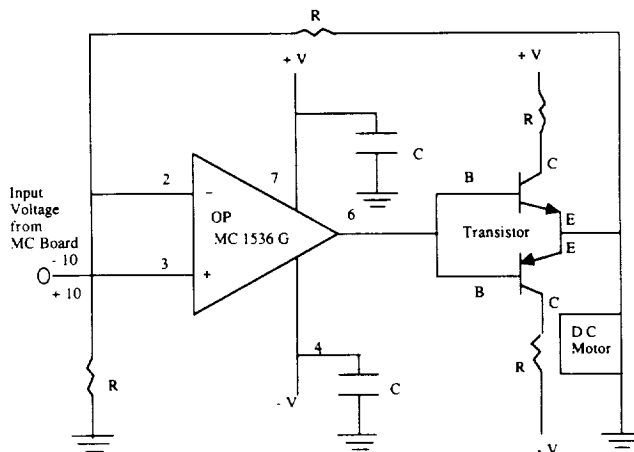

Fig. 14. Power Supply and Voltage Regulator

Two motion controller (MC) boards control the five DC motors on the arm. The MC-400 is able to control four motors while MC-200 can control two motors. The two MC boards are connected to the computer and wired to the motor drivers. Included in the package with the controller boards were two types of software: the "Stand Alone Program" aids in the installation and testing of the optical encoders, and the MC boards and the "Utility Subroutine and Program" aid in the development of a customer-written program. The software can be written in either "C" or "BASIC." The MC controller boards were accompanied by a user guide to assist in installation and operation. The block diagram for the control system is shown in Fig. 16.

The decision was made to use these MC boards over other possible choices because the controller cards were designed around the HCTL-1000 general-purpose Motion Control IC. The HCTL-1000 has the capacity to handle all encoder input decoding, phase commutation for steppers and brushless servomotors, digital filtering of the control signal, and generation of analog or pulse-width-modulated motor command signals. It continually performs intensive tasks of digital motion control, thereby freeing the PC for other planning tasks. The HCTL-1000 operation is controlled by a bank of 64 internal registers that, in turn, can be accessed by mapping within the PC memory. There is no need for interrupt-handling during operation.

To develop the control system, the robotic arm is viewed as a continuous time-varying system. The Laplace transform technique is used to simplify the analysis. The block diagram in Fig. 17 depicts the feedback closed-loop system of the robotic arm control. The digital controller is an IBM computer, while the DAC is a digital-to-analog converter, and the ADC is an analog-to-digital converter. The amplifier is the motor driver circuit used to convert the low-level analog torque signal u(t) to a voltage v(t), which directly activates the joint motors. Since the joints are DC motors, the generated torque is proportional to the armature current. Therefore, the amplifier in Fig. 17 is an analog subsystem regulating the

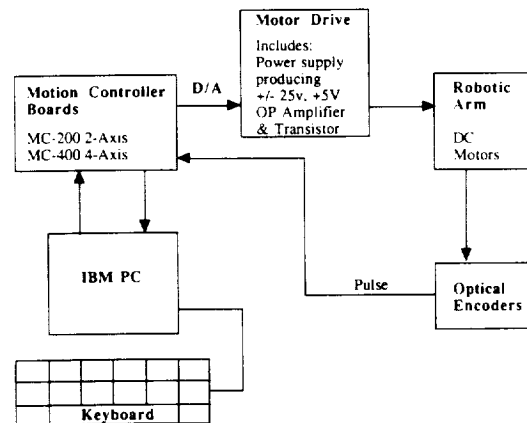Fig. 15. Circuit Design of Motor Driver

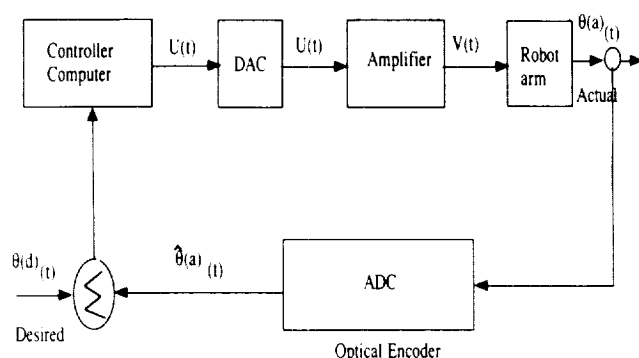Fig. 16. General Block Diagram for Robotic Arm Control System

Fig. 17. Feedback Closed Loop System of Digital Control

current through variations in the applied armature voltage. The ADC block detects the position (encoders) and the speed (tachometers) of the joint motors and converts them into a form recognized by the digital controller. Thus, the sensors here represent an encoded disk (optical encoder) of the type ADC.

The status of the project at this point is that we have control of four of the five motors on the arm. A program was written in "C" that can demonstrate a predetermined movement of the arm and its return. Since the initial (zero) position sensors are not installed, the arm can only be controlled using the joint coordinates. Two sample programs were developed for this purpose. One uses the voltage to control the joints. It reads and records the quadrature counts from the optical encoders. The second program uses the trapezoidal profile position control in an interactive mode. It has been modified to execute a sequence of point-to-point positions in the specified envelope. The user at this point may move all joints simultaneously or move one joint at a time to a predefined position. This requires only one keystroke to the keyboard.

Future Plan

The future plan of the software project is to move the arm with all 5 degrees of freedom integrating in a "pick-and-place" fashion. The arm will also be movable to any predetermined position in the physical envelope of the apparatus (i.e., move anywhere defined in polar (r,q) coordinates). Future work involves some hardware and software amplifications. For the hardware, some position sensors need to be installed for the initial (zero) position, and an optical encoder installed at the wrist. For the software aspect, the relationship between the inverse kinematics of the robot arm and the trajectory planning needs to be studied in more depth, and integration of the second arm must also be achieved. Components of this integration include state-of-the-art artificial intelligence and decentralized control algorithms. Additional considerations for the software portion include both error checking and recovery software that must be designed with the focal cutting point in mind as well as an initial (zero) position. All the above points must be intrinsic to the computer software each time

the machine is booted up or loaded. The future work of the project will take place in the succeeding semesters by other design teams.

MANIPULATOR ARM

The ASPOD spacecraft will need two robotic arms to successfully retrieve and process a piece of orbital debris. This year the task was to design and fabricate a new robotic arm. This arm was to be designed with the specific ASPOD mission in mind, and have the flexibility necessary for the handling of large pieces of debris.

Limitations

There will be no subsequent contact with the orbiter once it has been launched; therefore, it must be reliable. The arm must have a hand capable of grabbing most space debris as well as grappling with a larger satellite. Control of the arm must be precise. Vibrations, as well as slop/backlash within the arm's actuator mechanisms, must be minimized. The design must be adaptable to digital control and the electrical system must run off a 24-V power supply.

Design (Target) Specifications

In the process of generating alternative solutions the solar mirror structure was analyzed to determine the necessary DOFs. By approaching the problem in this manner, we would not have to analyze and build models to treat every design that did not have any immediate foreseeable problems. Analysis by this method led to a very unique solution.

First, it was determined that the easiest way to remove the lens from the holding slot was to translate it along an axis contained within the plane of the lens (see Fig. 18). We call this the hand axis from here on to clarify our discussion. Note that we assume the grasping mechanism to be attached to this axis.
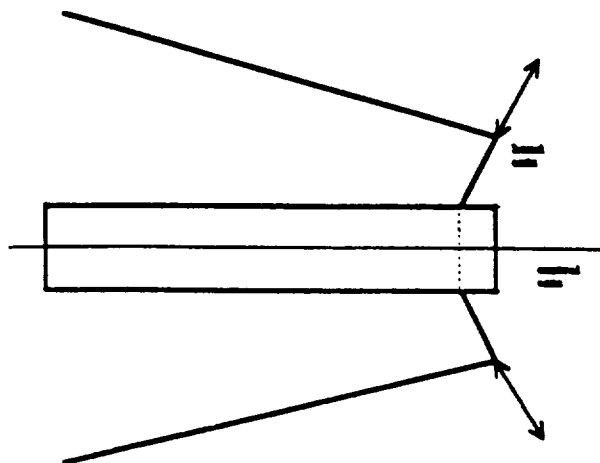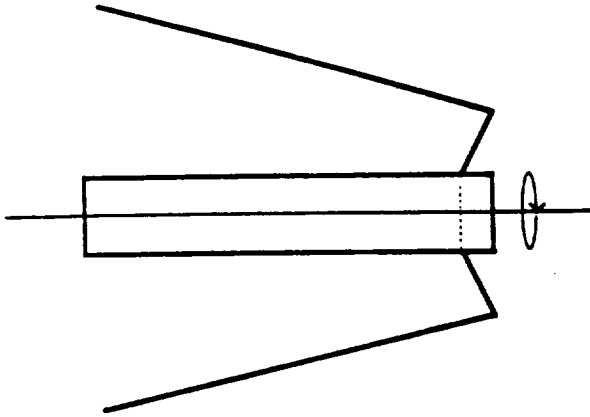

Fig. 18. Hand Axis

It is important to note that none of the DOFs required by the hand to perform properly have been considered here. The reason is that the DOFs discussed so far are for location and orientation of the hands—i.e., getting the hand to the desired locations—whereas the DOFs required by the hand are for orientation of the hand to receive the object. Those DOFs will be discussed in the subproblems involving the hand.

Using the three fundamental DOFs, the configuration in Fig. 21 was proposed. Note that the ring was used to accomplish the rotation about the central axis so that no part of the arm would be prone to moving through the focal point (see Figs. 21 and 22).

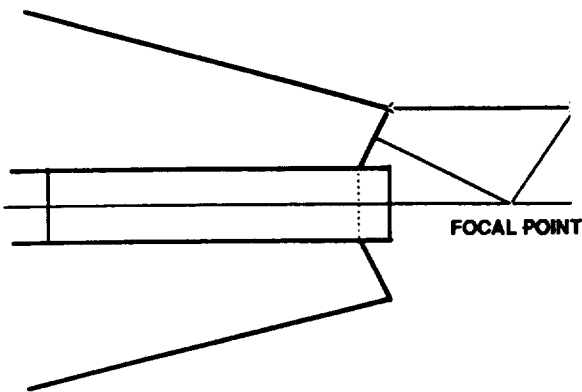Fig. 19. Central Axis Rotation

FOCAL POINT

Fig. 20. Focal Point Within Reach

Fig. 21.

To reach all three lenses with the hand axis in this orientation with respect to each lens individually, it is necessary to rotate about the central axis of the mirror structure (see Fig. 19).

The next requirement is for the arm to be able to reach the focal point. From Fig. 20 it can be seen that we need only to translate along an axis parallel to that of the central axis to meet this requirement. Finally, to reach debris located above the mirror structure the mechanism must be able to rotate about an axis perpendicular to the plane created by both the hand and central axis.

With these three DOFs we have a work area with roughly the shape of a cylinder with half spheres at the ends. Adding more DOFs in the form of joints or extensions would be redundant at this point. The adding of redundancies may decrease the difficulty of specific tasks. For example, in the case where an obstruction prevents the arm from directly reaching an object, it may be necessary to have another joint in the arm to essentially reach around the obstruction.
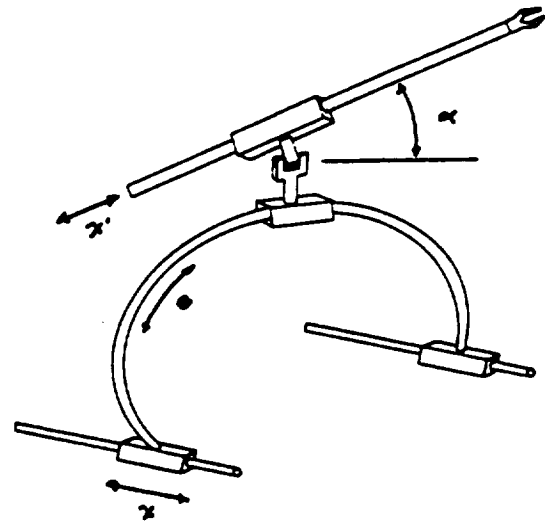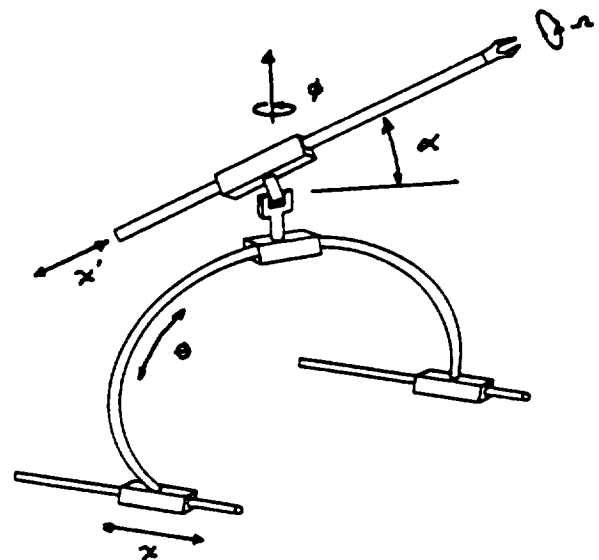

Fig. 22.

Final Design

Polar drive mechanism. The purpose of the axial tracks is to translate the entire robotic arm structure along the body of the collector. This is accomplished through motor driven screws. The motors have an output of 100 oz-in at 30 rpm per motor. This velocity will cause the polar track assembly to move at a rate of 4 in/min. The reason for keeping the velocity low is to prevent unwanted oscillations in the system. The power screws are regular 0.5 in and 13 threads per in.

The main load of the polar tracks is taken up by the bearings inside the pillow blocks. The bearings are 0.75-in linear bearings. Two linear bearings were used to prevent horizontal motion. The bearings ride on 60 case-hardened steel rods. This material was chosen because of its great stiffness capabilities and availability. Alongside the bearings, inside the pillow blocks, there are two couplings. The reason for using two is also to prevent horizontal deflection and to maximize the contact area between the pillow blocks and the driver screws.

The connection between the pillow blocks and the polar track is done through the flat plates that are welded to the polar track and the pillow blocks. The flat plates are bolted together.

The tracks, which were manufactured out of aluminum stock, are supported at the ends.

The circular track allows the arm to rotate about the focal point and align itself in a normal sense to the lens axis. The circular track allows the arm to access the mirror/lens structure without interference. A wide-base channel section (5 × 1.75-in cross-section) provides the necessary contact points to mount the arm and yields a "chamber" of space essential to the drive mechanism. The channel material is 5052 aluminum and initially weighed 24 lb. The weight was reduced to approximately 19 lb by drilling thirty 2.5-in diameter holes along the web, evenly spaced 3.5 in apart center to center. The holes did not weaken the track but did slightly deform it. The track's inside diameter was reduced by approximately 0.5 in, which is not a problem.

The arm is mounted onto the arm-platform, which contacts the channel track at six points: four on the outside and two on the inside. The rollers are Killian bearings that provide normal and lateral stability. The four outside bearings have been modified to prevent derailing. A washer has been pressed against the lip of the bearing. Two pairs of springs are incorporated in the design of the platform: one pair clamps the inside rollers to the platform providing normal stability, and the other pair ensures lateral contact of the bearings to the track. The springs are necessary to account for track irregularities.

The drive is simply a dual chain/sprocket drive. Power is transferred through a 50:1 worm gear reducer. The motor ordered was found to be faulty. It was rated at 10,000 rpm, 9 oz-in torque. Since it was to operate at shaft conditions of 500 rpm, 180 oz-in, this would give more than the needed torque of 500 oz-in. Testing showed motor output was nowhere near these specifications, so it was necessary to use a motor that was found and worked. No characteristics are known about the motor. Testing of the circular track drive

mechanism showed that operation performance was adequate for loads of 15 to 20 lb.

Elbow joint. The elbow joint provides one degree of freedom, which enables objects to be moved in or out of the focal point. It also supports access radially outward from the polar track providing access to objects that lie outside the ASPOD's framework. The elbow consists of two major components.

The first piece holds the motor and worm, and braces the 5/16-in shaft with a 7/8-in OD roller bearing press fit at either side. The selected motor is shown below as motor #1. The worm is steel, single-tooth, and 32 pitch. The shaft is held in place with snap rings.

The second major part of the elbow joint has a 32-pitch, 100-tooth worm wheel pressed into it. The worm wheel mates the worm on the first part when placed on the shaft. The shaft has a flat milled across it and is fixed to the worm wheel with a 5-40 set screw. The set screw is 2 in long so it not only holds the shaft but also fixes the wheel to the second piece.

Both parts of the elbow have a 1-in long hollow male fitting that is placed into a 1.5-in OD 0.0649-in thick pipe. All structural parts are made of aluminum; all fasteners are steel.

Motor rotor assembly. The motor rotor assembly is a gearbox that holds the arm above the polar track and allows the arm to rotate a full 360°. This provides access to objects in front, behind, or to either side of the ASPOD. The gearbox consists of two 9-in × 4-in plates separated 2.5 in by four spacers. The motor drives a 24-pitch, 100-tooth worm wheel that is held on the end of the shaft/endcap with 5-40 set screw. The motor selected for the gearbox is identified as motor #1. The motor is held at the precise height and angle with the motor mount.

The shaft/endcap is machined to have a 3/8-in shaft on one end and a 1/2-in long hollow male fitting on the other. It protrudes through the top of the gearbox so that the 1.5-in pipe that holds the elbow joint can be attached. The part of the endcap that joins the shaft was threaded with 9/32-in 18 threads/in. The shaft fits through a bearing and is held by a 9/32-in nut. The bearing is held in place with a machined cap. The cap was machined to have a snug fit with the bearing circumference and have a 1/1000-in interference fit between the bearing and top plate. The cap is fastened to the plate with four 6/32-in bolts.

Motor selection. The following motors were selected for their torque and speed. The exact weight was unknown but a rough estimate considering their size was also considered. The motors needed to have this great amount of torque as our initial estimates of the arm weight were too low. These motors will allow the arm to retain its original design capabilities of lifting a 2-lb plate at an extension of 33 in.

Motor #	Quantity	Torque (oz-in)	Speed (rpm)
1	2	100	375
2	1	25	1000
3	3	100	75
4	2	75	30

Grasping mechanism. The requirements of the grasping mechanism are that it must be able to grab a thin flat plate ranging in thickness from 0.125 to 0.75 in, grasp a cylinder with a diameter ranging from 0.125 to 4.0 in, and grasp a sphere with a diameter equal to that of the cylinder. Other general requirements for the mechanism are that the weight be minimal, the ratio of the clamping to the actuator force be maximized, and that the force ratio be as nearly constant throughout the range of motion of the mechanism as possible.

For the design that was developed and built to meet the requirements, the ratio of the clamping force to the actuator force is 0.25 and is nearly constant throughout the clamping range. The ratio was determined by constructing a static force vector diagram on each design at intervals in their range of motion. There was a trade-off between the increased ratio and smaller size. The force ratio would increase if the distance between the two sets of four bar linkages were increased. This design was chosen over five others because of its higher clamping force ratio, its smaller size, and its simplicity.

Harmonic vibrations. Vibrations of any space structure create special problems. The payload must be deployed, be able to precisely grab objects, and not suffer damage due to fatigue trying to capture satellites.

The space shuttle has a natural harmonic frequency of 32 Hz that prevents it from carrying a payload with a corresponding harmonic frequency less than or equal to 32 Hz. Such a payload (≤ 32 Hz) would certainly cause resonant vibrations of increasing amplitude. Damage to the shuttle resulting from resonance would be likely since it takes several hours to deploy any payload and the shuttle would be subject to the resonant vibrations until deployment since there is no damping in space.

If the robotic arm is to grasp an object, the exact position of the manipulator must be known. Low frequency vibrations tend to have greater amplitude and the end of the arm could move more than an inch. Use of space-rated composite materials (higher structural stiffness) would help to alleviate this problem.

If the amplitude of harmonic vibrations is too high, the robotic arm will experience high stresses. These stresses will cause fatigue damage if aluminum is the primary construction material of the arm. This is especially dangerous since space structures usually have little or no factor of safety. Composites have better fatiguing properties and should be used in all high-stress areas.

Conclusion. This year's research team designed and constructed the primary grappling arm. The arm has the ability to maneuver large and bulky objects into the focus of the Fresnel lens solar cutting device without obstructing the beam. A secondary function of the arm is to be able to repair or replace any of the Fresnel lenses if they are damaged. Both of these goals are met with the ASPOD robotic arm.

Most of the design specifications have been met. The arm can grasp a variety of objects from round balls to flat plates. It can be adapted to computer control by future design teams. All motors operate at 24 V (some are rated slightly higher but this presents no problem). The arm appears able to replace Fresnel lenses and repair the mirror array. However, the arm is not lightweight; in fact, it is so overweight that the Polar Arc is in distress. The arm is not reliable enough to operate for months or years without service.

Replacement of some aluminum parts with graphite composites would greatly enhance the performance of the robotic arm. Not only will weight be drastically reduced, but problems due to the low harmonics (4 to 10 Hz depending on its position) of the arm will be improved.

REFERENCES

1. Discover, December, 1988, p. 22.
2. GEO, March, 1989, p. 154.
3. Danish Science, December, 1988, p. 46.
4. Smithsonian, December, 1988.
5. Arizona Daily Star, February 21, 1987.
6. Tucson Citizen, February 27, 1987.
7. Arizona Republic, August 14, 1988.
8. Tucson Citizen, September 23, 1988.
9. American Way, May 15, 1989.
10. *Artificial Space Debris,* Johnson, Nicholas L., Orbit Book Company, Malabar, Florida, 1987.
11. Ibid
12. Ibid
13. Ibid
14. "Debris Danger Zone," Natural History, November, 1987.
15. "Hypervelocity Impact," NASA Activities, April-May, 1987.